STRUCTURAL BIOLOGY COMMUNICATIONS

Volume 74 (2018)

Supporting information for article:

Conformational changes with substrate binding revealed by structures of *Methylobacterium extorquens* malate dehydrogenase

Javier M. González, Ricardo Marti-Arbona, Julian C.-H. Chen, Brian Broom-Peltz and Clifford J. Unkefer

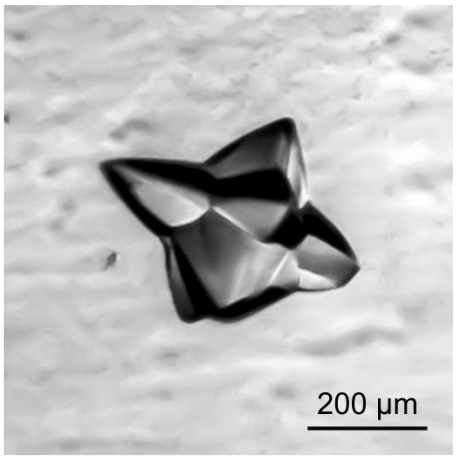

Figure S1 Crystal of *Mex*MDH.

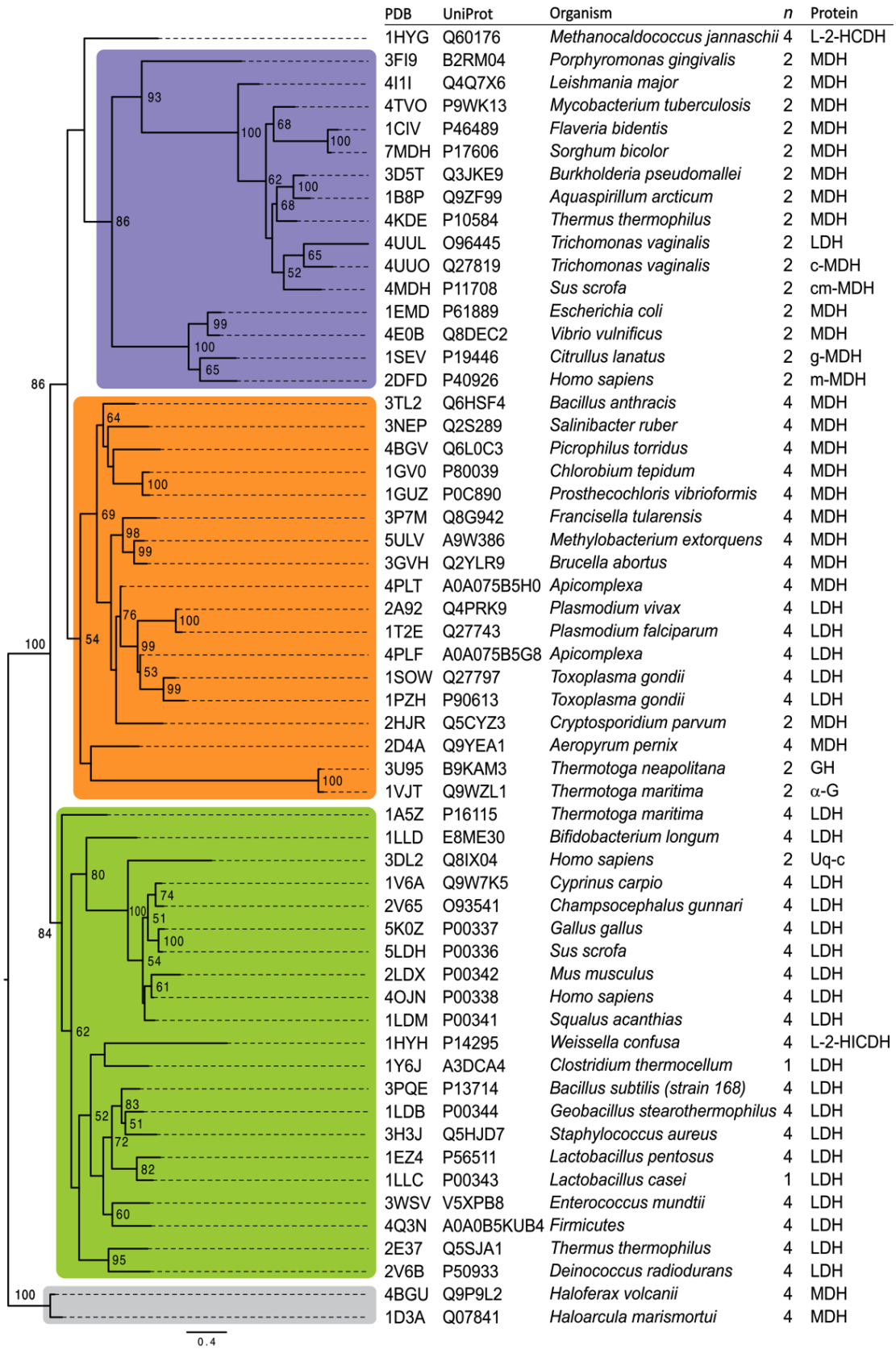
PDB UniProt Organism n Protein
1HYG Q60176 Methanocaldococcus jannaschii 4 L-2-HCDH
3FI9 B2RM04 Porphyromonas gingivalis 2 MDH
4I1I Q4Q7X6 Leishmania major 2 MDH
4TVO P9WK13 Mycobacterium tuberculosis 2 MDH
1CIV P46489 Flaveria bidentis 2 MDH
7MDH P17606 Sorghum bicolor 2 MDH
3D5T Q3JKE9 Burkholderia pseudomallei 2 MDH
1B8P Q9ZF99 Aquaspirillum arcticum 2 MDH
4KDE P10584 Thermus thermophilus 2 MDH
4UUL O96445 Trichomonas vaginalis 2 LDH
4UUO Q27819 Trichomonas vaginalis 2 c-MDH
4MDH P11708 Sus scrofa 2 cm-MDH
1EMD P61889 Escherichia coli 2 MDH
4E0B Q8DEC2 Vibrio vulnificus 2 MDH
1SEV P19446 Citrullus lanatus 2 g-MDH
2DFD P40926 Homo sapiens 2 m-MDH
3TL2 Q6HSF4 Bacillus anthracis 4 MDH
3NEP Q2S289 Salinibacter ruber 4 MDH
4BGV Q6L0C3 Picrophilus torridus 4 MDH
1GV0 P80039 Chlorobium tepidum 4 MDH
1GUZ P0C890 Prosthecochloris vibrioformis 4 MDH
3P7M Q8G942 Francisella tularensis 4 MDH
5ULV A9W386 Methylobacterium extorquens 4 MDH
3GVH Q2YLR9 Brucella abortus 4 MDH
4PLT A0A075B5H0 Apicomplexa 4 MDH
2A92 Q4PRK9 Plasmodium vivax 4 LDH
1T2E Q27743 Plasmodium falciparum 4 LDH
4PLF A0A075B5G8 Apicomplexa 4 LDH
1SOW Q27797 Toxoplasma gondii 4 LDH
1PZH P90613 Toxoplasma gondii 4 LDH
2HJR Q5CYZ3 Cryptosporidium parvum 2 MDH
2D4A Q9YEA1 Aeropyrum pernix 4 MDH
3U95 B9KAM3 Thermotoga neapolitana 2 GH
1VJT Q9WZL1 Thermotoga maritima 2 α-G
1A5Z P16115 Thermotoga maritima 4 LDH
1LLD E8ME30 Bifidobacterium longum 4 LDH
3DL2 Q8IX04 Homo sapiens 2 Uq-c
1V6A Q9W7K5 Cyprinus carpio 4 LDH
2V65 O93541 Champsocephalus gunnari 4 LDH
5K0Z P00337 Gallus gallus 4 LDH
5LDH P00336 Sus scrofa 4 LDH
2LDX P00342 Mus musculus 4 LDH
4OJN P00338 Homo sapiens 4 LDH
1LDM P00341 Squalus acanthias 4 LDH
1HYH P14295 Weissella confusa 4 L-2-HICDH
1Y6J A3DCA4 Clostridium thermocellum 1 LDH
3PQE P13714 Bacillus subtilis (strain 168) 4 LDH
1LDB P00344 Geobacillus stearothermophilus 4 LDH
3H3J Q5HJD7 Staphylococcus aureus 4 LDH
1EZ4 P56511 Lactobacillus pentosus 4 LDH
1LLC P00343 Lactobacillus casei 1 LDH
3WSV V5XPB8 Enterococcus mundtii 4 LDH
4Q3N A0A0B5KUB4 Firmicutes 4 LDH
2E37 Q5SJA1 Thermus thermophilus 4 LDH
2V6B P50933 Deinococcus radiodurans 4 LDH
4BGU Q9P9L2 Haloferax volcanii 4 MDH
1D3A Q07841 Haloarcula marismortui 4 MDH
0.4

Figure S2 Maximum-likelihood phylogenetic tree of all the MDH/LDH-like proteins available in the Protein Data Bank, filtered with a 90 % identity cutoff. The three main clades comprise dimeric malate dehydrogenases (*purple*), tetrameric malate dehydrogenases (*orange*), and tetrameric lactate dehydrogenases (*green*). Note that dimeric LDH enzymes are unusual. Bootstrap node support values are indicated as percent for nodes with ≥ 50 % support. The acronyms stand for: malate and lactate dehydrogenase (MDH, LD); L-2-hydroxycarboxylate dehydrogenase (L-2-HCDH); cytosolic-, cytoplasmic-, glyoxysomal-, mitochondrial-MDH (respectively c-, cm-, g-, and m-MDH); glycoside hydrolase (GH); α-glucosidase (α-G); and L-2-hydroxyisocaproate dehydrogenase (L-2-HICDH). The divergent MDH enzymes from *Haloferax volcanii* and *Haloarcula marismortui* were selected as outgroup (*gray*).

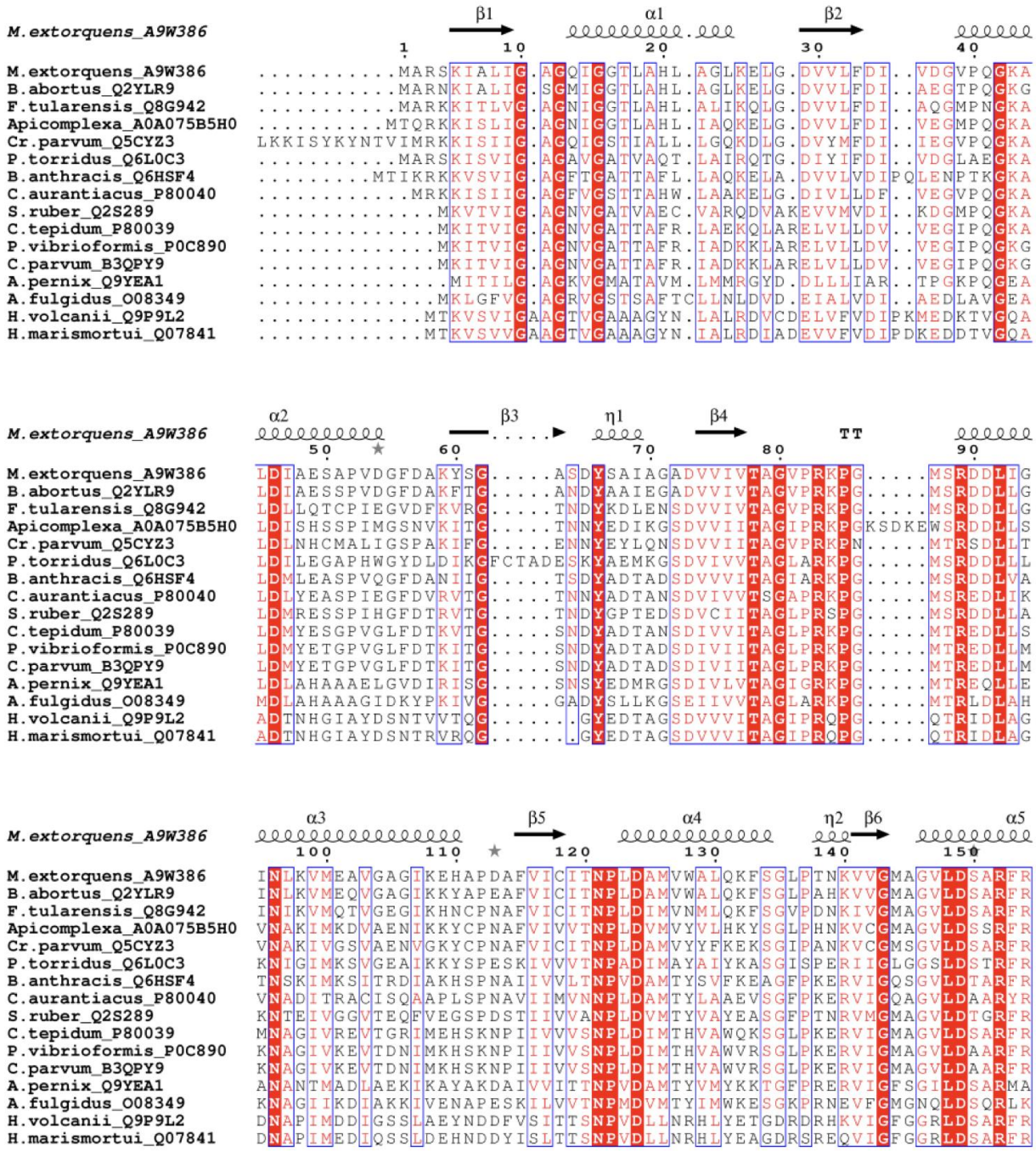
M.extorquens_A9W386
M.extorquens_A9W386
B.abortus_Q2YLR9
F.tularensis_Q8G942
Apicomplexa_A0A075B5H0
Cr.parvum_Q5CYZ3
P.torridus_Q6L0C3
B.anthracis_Q6HSF4
C.aurantiacus_P80040
S.ruber_Q2S289
C.tepidum_P80039
P.vibrioformis_P0C890
C.parvum_B3QPY9
A.pernix_Q9YEA1
A.fulgidus_O08349
H.volcanii_Q9P9L2
H.marismortui_Q07841

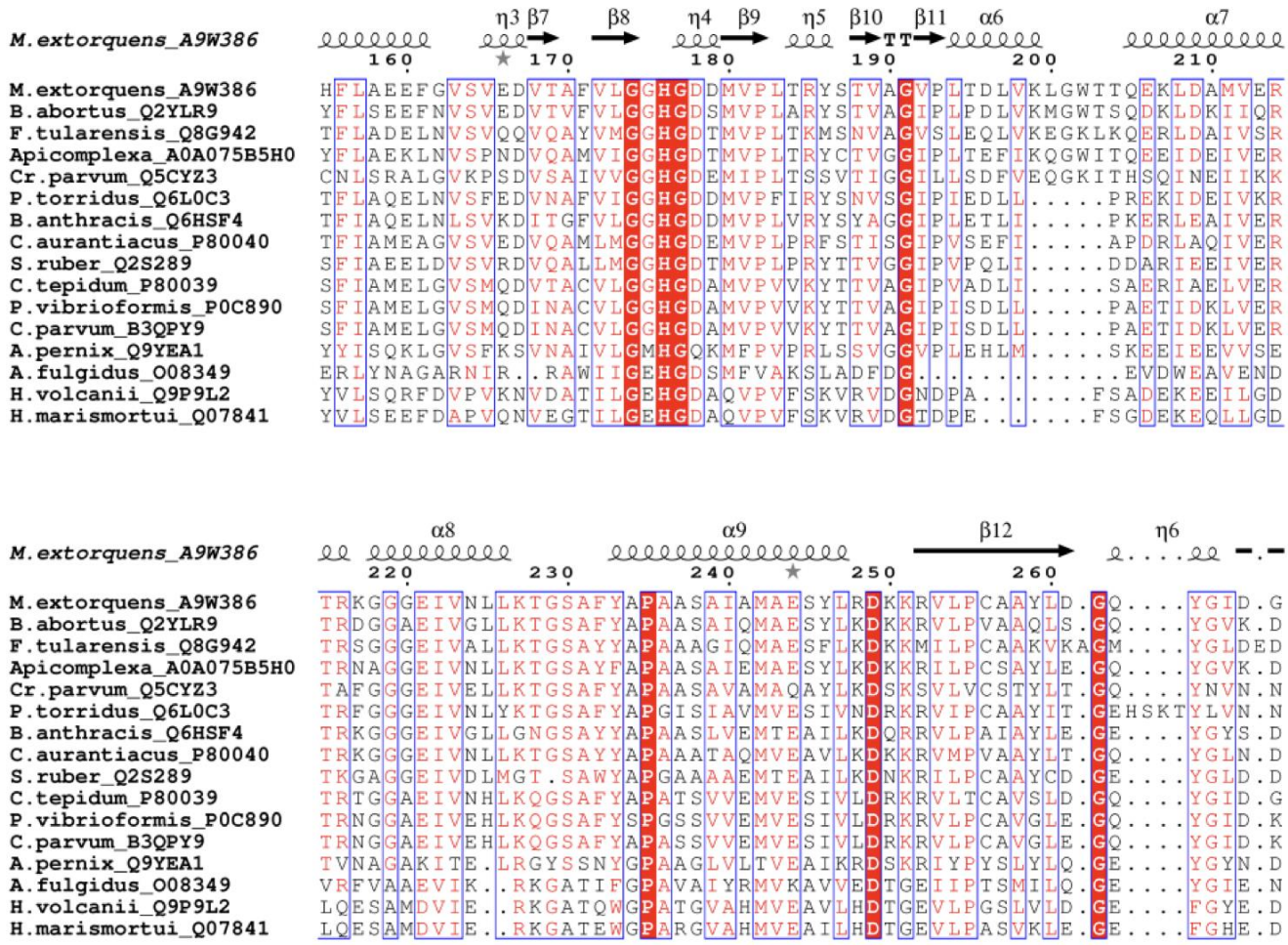

Figure S3 Sequence alignment of selected MDH enzymes. The indicated alphanumeric codes for each microorganism name indicate the corresponding sequence ID for the UniProtKB database. Graphical representation was prepared with ESPRIPT (available at http://espript.ibcp.fr). See the main text for additional details.

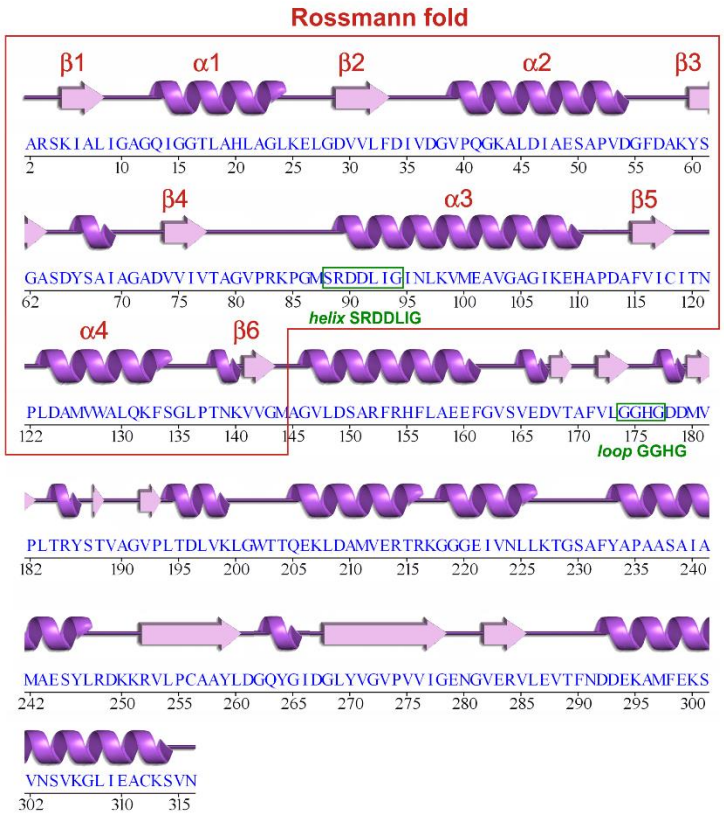

Figure S4 Topological arrangement of *Mex*MDH secondary structure elements. The image was prepared with the structure PDB 5luv (reported in this work), based on the output of PDBSUM (available at http://www.ebi.ac.uk/thornton-srv/databases/pdbsum/).

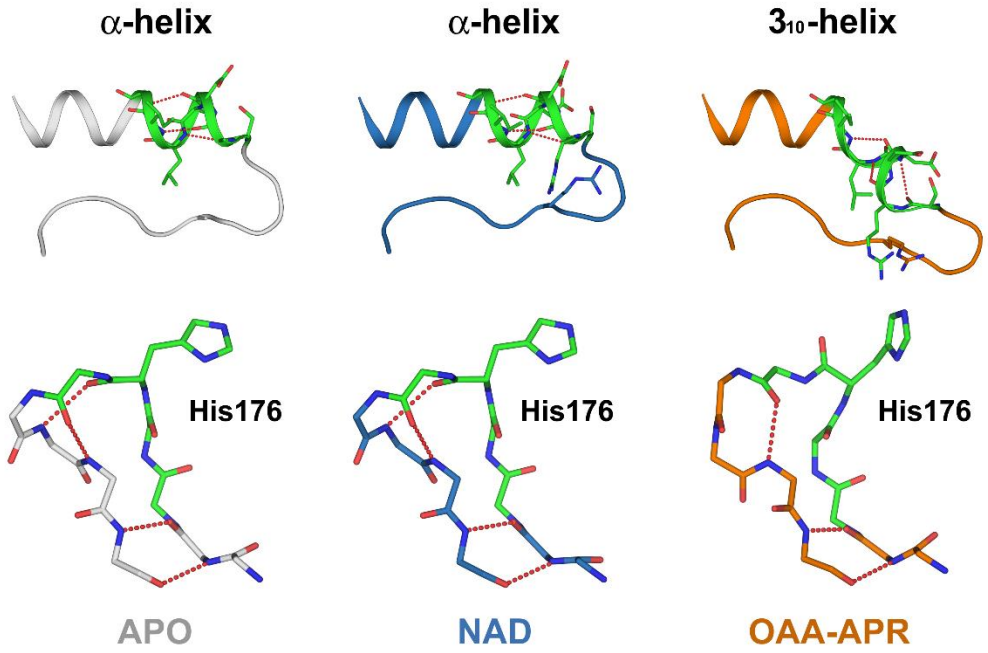

Figure S5 Cartoon representation of the conformational changes associated with NAD binding (*blue*) and OAA-APR binding (*orange*) as compared with the apo-enzyme resting state (*gray*). OAA induces the most important conformational changes (highlighted in *green*) in helix SRDDLIG (experiencing a transition between α-helix and 3_{10}-helix), and loop GGHG.

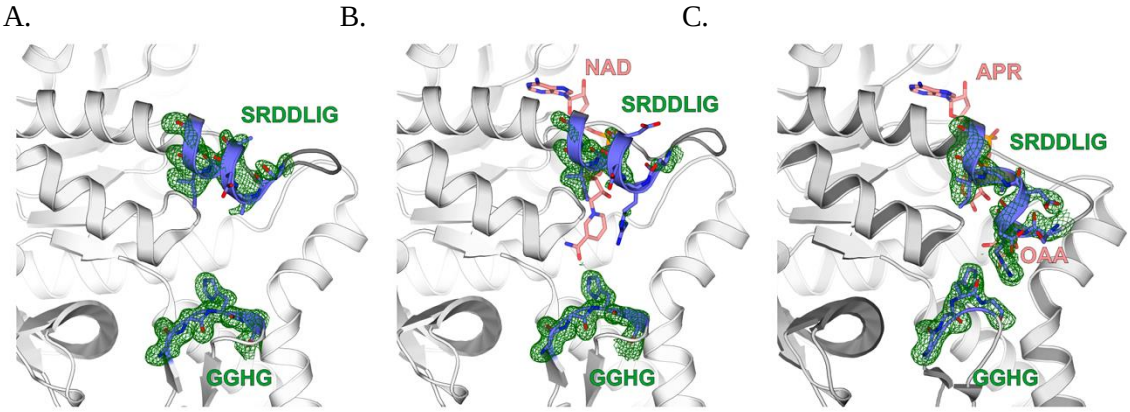

Figure S6 Polder OMIT maps (Liebschner *et al.*, 2017) for loops SRDDLIG and GGHG. (*a*) Apo, (*b*) NAD, and (*c*) OAA-APR *Mex*MDH. Relevant areas are colored in *blue*, with polder maps in *green*, and ligands in *pink*. Polder maps were calculated with Phenix 1.13-2998, contoured at 2.5 r.m.s.d. Figures were prepared with PyMOL 1.8.3.2 (Schrodinger) and Corel Draw X7 (Corel).